8 Hottel, H. C., and Sarofim, A. F., *Radiative Transfer*, McGraw-Hill, New York, 1967.
9 Felske, J. D., and Charalamopoulos, T. T., "Gray Gas Weighting Coefficient for Arbitrary Gas-Soot Mixtures," *Int. J. Heat Mass Transfer*, Vol. 25, 1928, pp. 1849–1855.
10 Al-Turki, A. M., and Smith, T. F., "Emissivity and Absorptivity of Gas-Soot Mixtures," Technical Report E-TFS-84-003, Department of Mechanical Engineering, The University of Iowa, 1984.
11 Smith, T. F., Shen, Z. F., and Friedman, J. N., "Evaluation of Coefficients for the Weighted Sum of Gray Gases Model," ASME JOURNAL OF HEAT TRANSFER, Vol. 104, 1982, pp. 602–608.
12 Beier, R. A., and Pagni, P. J., "Soot Volume Fraction Profiles in a Forced-Combusting Boundary Layers," ASME JOURNAL OF HEAT TRANSFER, Vol. 105, 1983, pp. 159–165.

Quenching of a Hollow Sphere

S. Subramanian[1] and L. C. Witte[2]

Introduction

Most analyses of boiling on cylinders and spheres assume uniform surface temperature. For bodies that are small or have high conductivity, this is a fair assumption. But for large bodies, the variation of heat flux q around the body might be large enough to cause significant variations in temperature T on a surface that cannot provide unlimited energy to the boiling process by internal conduction. As an example, Ungar and Eichhorn [1] measured large T variations around a 2.54-cm copper sphere quenched in methanol. Such T variation led to nonuniform boiling regimes around the sphere and cast doubt about the significance of minimum and maximum heat fluxes that one would calculate from experiments where T uniformity is assumed. Thibault and Hoffman [2] also measured large variations in heat flux about a 12.7-cm copper cylinder quenched in water.

A hollow sphere, used in this study, removes the conduction path from the front to the back of the body; therefore any spatial variations in heat flux would enhance the T variation in the angular (θ) direction around the body. The output of two thermocouples (TC) mounted inside the sphere was linked to the boiling behavior on the surface by using a specially designed timing circuit that provided simultaneous timing marks for the T–t records and for high-speed motion pictures of selected experiments.

Apparatus

Figure 1 shows the 2.54-cm hollow sphere; it was machined in two parts that were press-fitted together after installation of the thermocouples. The press-fit seam was silver-soldered to eliminate contact resistance between the two halves. The TC beads were peened and silver-soldered into depressions machined into the inner surface. Additional details of the sphere's construction are given in [3].

Following heating in an electric furnace, the sphere was quenched in methanol and water contained in a transparent tank equipped with an immersion heater. The TC outputs and timing signals were recorded on a Tektronix 565 oscilloscope. The timing pulses were also fed to the timing LED channel of a Photec IV high-speed camera used to photograph selected experiments. The details of the timing circuit are given in [3].

Data Reduction

Significant T variations occurred around the sphere during transition/nucleate boiling. Thus the T–t data had to be reduced so as to account for T and q variation in the θ direction, as follows: The sphere was split into nine azimuthal rings for a finite-difference calculation of the local heat fluxes. The input to the calculational model was a third-order polynomial curve-fit of the temperature variation around the sphere at discrete points in time. The four boundary conditions

$$\theta = 0 \qquad dT/d\theta = 0$$
$$\theta = 45 \text{ deg}, \qquad T = \text{TC1}$$
$$\theta = 135 \text{ deg}, \qquad T = \text{TC2}$$
$$\theta = 180 \text{ deg}, \qquad dT/d\theta = 0$$

were used. The finite difference model accounted for the energy flowing around the periphery of the sphere as well as for the loss of internal energy of any particular element. The details of the model are omitted for brevity, see [3]. An uncertainty analysis showed that the maximum uncertainty of ±5 percent for calculated q occurred in the transition/nucleate boiling regime.

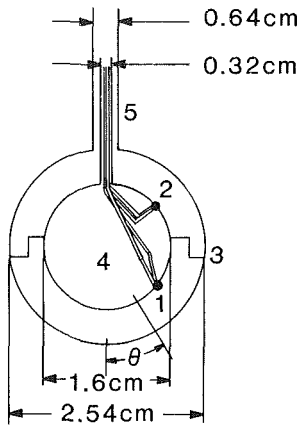

1. TC1, θ = 45°
2. TC2, θ = 135°
3. Silver soldered equator
4. Ceramic bead insulation
5. Support stem

Fig. 1 Schematic diagram of the test sphere

Discussion of Results

Over 100 trials involving methanol and water were made. Twenty-eight of the methanol tests were used for data reported herein. The remainder were used for repeatability verification and apparatus checkout. All tests reported herein were performed with the bottom of the sphere immersed 3.81 cm below the surface of the methanol.

Figure 2 shows the T–t history and the fluxes calculated for the TC1 and TC2 locations for 24°C methanol. This test included motion pictures taken at 800 frames/s. Figure 2 will be used to explain the general nature of subcooled methanol boiling. Motion pictures of boiling subcooled water showed the same qualitative behavior as observed in methanol.

Physics of Subcooled Quenching. Near the end of film boiling, when the sphere was virtually at uniform T, some sort of disturbance originated on the liquid–vapor interface at the right-hand side of the sphere and propagated rapidly over the sphere surface. It is shown by sketch B on Fig. 2. The frame number (1918) when the disturbance started is also shown on

[1]Research Assistant, University of Houston, Houston, TX 77004.
[2]Professor, Department of Mechanical Engineering, University of Houston, Houston, TX 77004; Fellow ASME.
Contributed by the Heat Transfer Division for publication in the JOURNAL OF HEAT TRANSFER. Manuscript received by the Heat Transfer Division April 1, 1985.

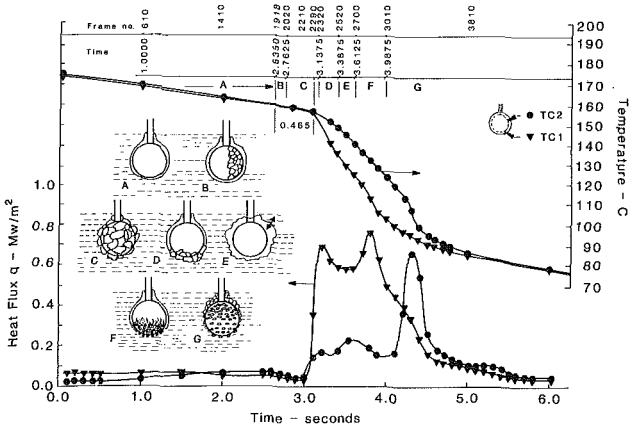

Fig. 2 Plot of heat flux and temperature histories for methanol at 24°C

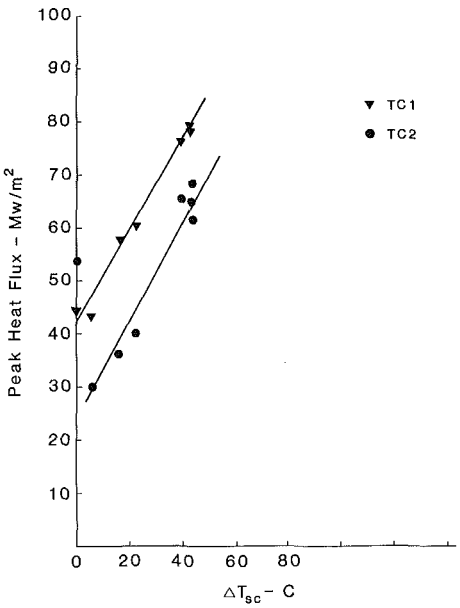

Fig. 3 Peak heat fluxes versus subcooling for methanol

the figure. Once it fully covered the sphere (0.1275 s later), a distinctly different type of liquid-vapor interface developed, which we called "randomly rippled," shown in sketch C. There was a 0.465 s lag between the beginning of the disturbance and when the TCs registered a significant drop in temperature. The characteristic conduction time for the sphere was 0.044 s, so although the TCs could have responded to the disturbance, they did not do so until almost 10 time constants later. This implies that the disturbance was confined to the liquid-vapor interface itself rather than causing massive liquid-solid contact that would have quickly caused a drop in surface temperature.

The sharp drop in TC1 was precipitated by a collapse of the vapor film beginning at the bottom of the sphere at about frame 2320. It is shown as sketch D on the figure. It was relatively violent and quickly set the vapor film into an oscillatory motion. Once this collapse began, the boiling behavior around the sphere became highly localized, as demonstrated in Fig. 2 by the differences in q at TC1 and TC2. The localized nature of the boiling persisted throughout the transition and most of the nucleate boiling regimes.

The oscillations of the vapor film that followed the vapor film collapse led to a decrease in the heat fluxes, especially for TC1, which shows a distinct lessening of the cooling rate between frames 2500 and 2600. Eventually, a nucleate boiling "front" moved around from the bottom to the top of the sphere, as shown in sketch F. Three regimes of boiling might coexist on the sphere at once: nucleate at the bottom, film at the top, separated by an oscillating transition boiling "ring."

The peak heat flux clearly propagated from the bottom to the top of the sphere. The peak heat flux was highest for TC1, which experienced it first. In fact, *all* experiments showed that the peak heat flux was highest for the TC location that experienced it first. Although separated in time on Fig. 2, the peak heat fluxes for TC1 and TC2 occurred at about the same temperature.

Effect of Subcooling. The collapse of the vapor film was much faster for subcooled than for saturated methanol. Subcooled methanol always exhibited "dual maxima" in its boiling curves as shown in Fig. 2. This is indicative of the highly localized nature of transition boiling around the sphere. The first maxima abated as the methanol was brought toward saturation.

Peak Heat Fluxes. Figure 3 shows that nucleate peak heat fluxes (second maximum) were strongly dependent upon liquid subcooling. There was an increase in peak heat flux with subcooling (ΔT_{sc}) for both TC locations. For saturated methanol, the top TC experienced the peak heat flux first, i.e., the vapor film collapsed at the top first and then moved downward over the sphere. In *all* tests the TC that experienced the peak flux first gave the highest value. As subcooling was imposed, the vapor film collapsed at the bottom first thus reversing the TC location where peak flux was highest.

Thibault and Hoffman [2] found that the highest peak heat flux occurred at the top of a 12.7-cm copper cylinder quenched in saturated water. As subcooling increased, the peak heat flux increased more rapidly over the lower parts of the cylinder than at the top, which is in basic agreement with our observations. Ded and Lienhard's [4] theory for peak heat flux agreed to within 5 percent of our average measured values for saturated methanol.

Conclusions

The major findings in this study are:

1 The TC location that experienced it first always gave the highest peak heat flux. When the transition front reached the second TC location, energy had been removed from that location by adjacent points which had already experienced the peak heat flux, thus limiting the amount of energy that could be provided to the boiling process.

2 Double maxima were observed for subcooled boiling. The first maximum corresponded to the initial collapse of the vapor film, while the second represented the nucleate peak heat flux regime. Between the two maxima, a vapor envelope oscillated locally over the surface.

3 Saturated boiling was more global than was subcooled boiling, but the peak heat flux was not uniformly distributed. The average saturated peak heat flux was predicted well by Ded and Lienhard's global theory.

4 All three regimes of boiling – film, transition, and nucleate – might coexist on the surface studied herein. Such behavior became more pronounced as subcooling was increased.

5 T variation around the sphere was virtually nil for film boiling. Consequently, analyses of film boiling assuming uniform T distribution should be adequate even for highly subcooled conditions.

References

1 Ungar, E., and Eichhorn, R., "Local Surface Boiling Heat Transfer From a Submerged Sphere," ASME Paper No. 82-HT-27.

2 Thibault, J., and Hoffman, T. W., "Local Boiling Heat Flux Density Around a Horizontal Cylinder," *Proc. 6th Int. Heat Transfer Conference*, Toronto, 1978, pp. 199–204.

3 Subramanian, S., "Quenching of a Hollow Sphere," MS Thesis, Department of Mechanical Engineering, University of Houston, Houston, TX, Dec. 1984.

4 Ded, J. S., and Lienhard, J. H., "The Peak Pool Boiling Heat Flux From a Sphere," *AIChE J.*, Vol. 18, No. 2, 1972, p. 337.

Depressurization Experiment in a Sodium-Heated Steam Generator Tube

D. M. France[1,2] and R. D. Carlson[1]

1.0 Introduction

Large-capacity steam generators for electric power plants are designed to operate over a wide range of conditions, including normal and off-normal steady-state loads and plant transients. Several shutdown transients for liquid metal fast breeder reactor (LMFBR) power plants were analyzed with the DEMO computer code [1]; results were presented in [2].

One of the more severe transients for the steam generators is the "waterside isolation and dump" transient, which is a planned transient designed into the plant control system. As explained in [2], the purpose of the transient is to minimize the water inventory in the steam generator during a sodium–water reaction resulting from a tube or weld leak. The transient is initiated by closing water valves at the steam generator inlet and outlet thus isolating it from the remainder of the water circuit. Other valves are opened, allowing the isolated water in the steam generator to flow into auxiliary vessels at atmospheric pressure. This sequence of events results in relatively fast depressurization and removal of the water in the steam generator and is often termed the "blowdown" transient.

A blowdown experiment was performed in this study using a sodium-heated test section with geometry and parameters typical of LMFBR steam generators. Water boiling inside a tube at 16 MPa was depressurized to atmospheric pressure in 30 s with the objective of determining the severity of the transient in terms of flow, temperature, and pressure gradients. The experiment was unique in terms of the full-scale test section size, the high pressures and temperatures, and the speed of the depressurization. Quantitative results presented show that the very large pressure and flow gradients that occur are confined to the initiation stage of the transient where system control could be used to mitigate the severity.

2.0 Experimental Analysis

Experiments were performed at Argonne National Laboratory-East in the Steam Generator Test Facility (SGTF). The facility has a nominal power rating of 1 MW and is designed to test full-scale LMFBR steam generator tubes at conditions prototypic of plant operation. The facility is described in detail in [3, 4].

The test section consisted of a single-tube shell and tube heat exchanger mounted vertically. Subcooled water entered the bottom of the tube and flowed upward as it was heated by sodium flowing countercurrent in the shell. The test section is shown schematically in Fig. 1. The dimensions and material of the heat transfer tube are given in the figure.

Two types of thermocouples are depicted in Fig. 1. The shell thermocouples were used in the present experiments to calculate axial heat flux, water temperature, and water quality distributions before initiation of the transient. The internal thermocouples, which were embedded in the wall of the heat transfer tube, were used during the transient to indicate the movement of liquid in the tube.

The test section inlet and exit piping arrangements are shown in Fig. 2. A single valve at the steam outlet from the test section isolated the top of the test section from the remainder of the water circuit; two valves were used for this purpose at the water inlet. Two blowdown valves were used, one each at the water inlet and outlet, to allow water to flow to the atmosphere from the test section water tube. The test section outlet isolation valve is numbered WV3A; the outlet blowdown valve is located between the test section exit and this valve. The test section inlet was isolated by closing both valves WV2 and WV6. The inlet blowdown valve was located between these two valves and the test section inlet, and the water flowmeter was located between the inlet blowdown valve and the test section inlet, as shown in Fig. 2.

The pressure and temperature of the water flow were measured close to the inlet and exit of the test section, as indicated by "*T*,*P*" in Fig. 2. Linear displacement transformers were placed on the isolation and blowdown valves to monitor positions as a function of time during the transient. The tran-

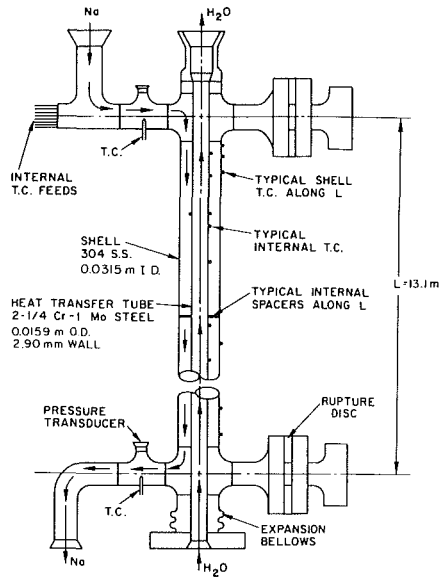

Fig. 1 Test section

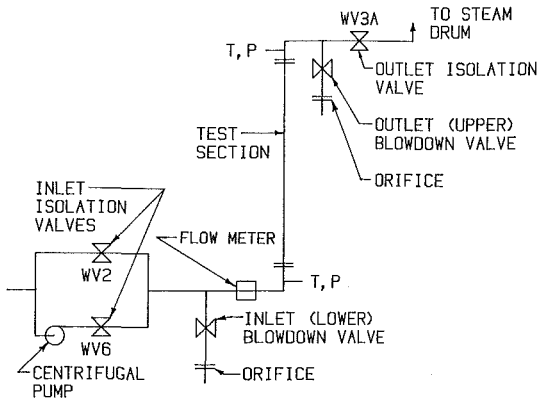

Fig. 2 Water valve arrangement

[1]Argonne National Laboratory, Components Technology Division, Argonne, IL 60439.

[2]Currently at University of Illinois at Chicago, Department of Mechanical Engineering, Chicago, IL 60680, USA; Mem. ASME.

Contributed by the Heat Transfer Division for publication in the JOURNAL OF HEAT TRANSFER. Manuscript received by the Heat Transfer Division January 17, 1985.